

CORE-SHELL STRUCTURES AND PRECIPITATION KINETICS OF $\text{Al}_3(\text{Sc}, \text{Zr})\text{Li}_2$ INTERMETALLIC PHASE IN Al-RICH ALLOY

V. RADMILOVIC¹, A. TOLLEY^{1,2},
Z. LEE¹, and U. DAHMEN¹

¹ National Center for Electron Microscopy, Lawrence Berkeley National
Laboratory, University of California, 1 Cyclotron Road, Berkeley, CA 94720,
USA; ZHLee@lbl.gov, UDahmen@lbl.gov

² Centro Atómico Bariloche, Comisión Nacional de Energía Atómica and CONICET,
Av. Bustillo 9500, San Carlos de Bariloche, 8400 Río Negro,
Argentina; tolley@cab.cnea.gov.ar

ABSTRACT

While binary Al-Sc alloys form Al_3Sc intermetallic precipitates, ternary Al-Sc-Zr alloys develop precipitates that contain both Sc and Zr. Electron microscopy characterization using Z-contrast imaging indicates rapid initial formation of $\text{Al}_3(\text{Sc}, \text{Zr})$ precipitates with a Sc-rich core followed by the slower development of a Zr-rich $\text{Al}_3(\text{Zr}, \text{Sc})$ shell. The shell acts as a diffusion barrier, slowing down the rate of precipitate coarsening.

Key words: Al-Sc-Zr alloys, Coarsening, Core/shell precipitates, TEM, STEM

INTRODUCTION

Core-shell particle structures have received considerable attention because it has been demonstrated that the shell can significantly alter the core properties. Our investigation of an Al-Sc-Zr alloy has shown that a core-shell structure may be responsible for the modification of properties in a precipitate-hardened alloy system. The addition of Sc and Zr to aluminum alloys usually results in improved mechanical properties, primarily alloy strength because Sc is the most potent strengthening alloying element for Al based alloys [1, 2]. Sc and Zr form Al_3Sc or Al_3Zr precipitates that pin grain boundaries, improve recrystallization resistance of Al alloys, and also contribute to their hardening [3, 4]. Al-Sc based alloys are also candidates for applications in aerospace and transport industries because of superior creep properties [5]. It has been shown that the solid solution of Sc in Al decomposes at a rate which is more than 3 to 4 orders of magnitude higher than the corresponding rate for Al-Zr alloys [6]. The same authors suggested addition of Zr to binary Al-Sc alloy to slow down precipitation kinetics [7].

Our recent work on Al-Sc-Zr alloys [8] has shown that Al_3Sc or Al_3Zr precipitates develop a core/shell structure during aging at 450°C. We demonstrated that the

precipitates contained both Sc and Zr, but that the distribution of Zr and Sc was not homogeneous. Instead, a Zr-rich shell surrounded a Sc-rich core. These complex precipitates may be responsible for the modification of properties in Al based precipitate-hardened alloy systems. Therefore, detailed understanding of the precipitation process is necessary for alloy design.

In this work, the precipitation processes of binary Al-Sc and ternary Al-Sc-Zr are compared using transmission electron microscopy for a detailed characterization of the structure, morphology and composition of the precipitates and the kinetics of precipitation in the ternary alloy.

EXPERIMENTAL DETAILS

Binary Al-Sc and ternary Al-Sc-Zr alloys with the same Sc content were prepared by arc melting. The composition of the alloys, determined by atomic emission spectroscopy was: Al-0.61wt%Sc and Al-0.61wt%Sc-0.40wt%Zr, respectively. Both alloys were homogenized simultaneously in separate quartz tubes back-filled with a low Ar pressure at 640°C for 24 hours. They were quenched into a mixture of ice and water at 0°C. Slices of the homogenized alloys were aged together at 300°C, 350°C, 400°C and 450°C in an electrical resistance furnace and quenched into water at room temperature. Samples in the shape of discs with 3mm diameter for characterization by transmission electron microscopy (TEM) were cut from the foils, and thinned to electron transparency by electropolishing with an 8% sulfuric acid, 2% hydrofluoric acid, 5% glycerol, 85% methanol electrolyte at -25°C. The evolution of precipitate size was studied using JEOL 200 CX, Philips CM200FEG, and TECNAI F20 UT microscopes. Particle sizes were measured from dark field images using the 110-type superlattice reflections of the precipitates. Over 150 particles were analyzed manually for each size determination. Foil thickness for the determination of precipitate number density was measured from the position of dark fringes in a 220 two beam convergent beam diffraction pattern. Precipitate densities were determined by visually counting precipitates within a determined area, and dividing by the local volume. High angle annular dark field (HAADF) Z-contrast images were obtained close to or on the 001 zone axis. Differential scanning calorimetry was performed using a TA Instruments Q1000 DSC at heating rates of 5, 10, 20 and 30°Cmin⁻¹ in the temperature interval 40-500°C with an aluminum crucible in a dry argon atmosphere.

RESULTS AND DISCUSSION

Fig. 1 shows the evolution of the precipitate mean radius as a function of annealing time and annealing temperature at 300, 350, 400 and 450°C for binary Al-Sc and ternary Al-Sc-Zr alloys. During the initial stages of annealing at each temperature, the size of the precipitates in Al-Sc is smaller than that in the ternary alloy. However, due to slower coarsening of precipitates in the ternary alloy, after prolonged annealing the ternary Al-Sc-Zr alloy precipitates are smaller than those in binary Al-Sc. In fig. 1, it can also be seen that in binary Al-Sc, the cube of the mean radius increases linearly as from the very initial stages. By comparison, in the ternary alloy, the cube linear relationship exists only for the later stages of precipitation, but a departure from this relationship is observed during the initial stages (most clearly seen at 300 and 350°C).

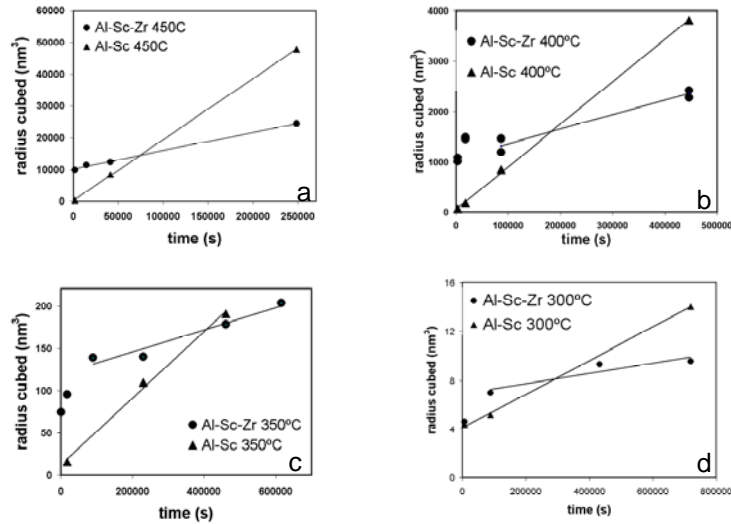


Fig. 1: Plots of r^3 vs t in binary Al-Sc and ternary Al-Sc-Zr for coarsening analysis. a) 450°C, b) 400°C, c) 350°C, d) 300°C.

Fig. 2 shows dark field images of both alloys at the initial stage (5h) and late stage (124h) of annealing at 400°C. The reduced rate of coarsening is clearly apparent. Fig. 3 compares the evolution of precipitate number density as a function of annealing time in the binary and ternary alloys. During the initial aging stage, the number density in the ternary alloy is significantly lower than that in binary Al-Sc. Furthermore, whereas number density decreases monotonically in the binary alloy, in the ternary alloy it initially increases, goes through a maximum and then decreases. These effects could be due to a smaller supersaturation in the ternary alloy, which reduces the nucleation rate. The linear fits of the ternary alloy data in Fig. 1 correspond to the later aging stages where the number density is decreasing.

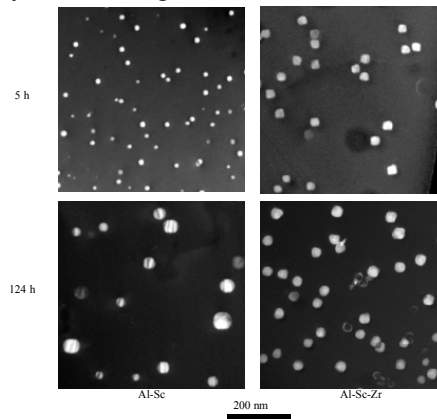


Fig. 2: Comparison of precipitate size at initial and late stages of annealing at 400°C.

It is obvious from figures 1-3 that the addition of Zr to the binary Al-Sc strongly affects the precipitate evolution. During the initial stages of precipitation, higher growth rates are observed in the ternary alloy, resulting in larger precipitates. In the later stages

of annealing, Zr strongly reduces the coarsening rate of precipitates. This effect is apparent in figure 1, where a lower slope in the r^3 vs t plots is clearly seen in the ternary alloy. Such a reduction has also been observed by small angle X-ray scattering [9]. This effect is related to the Zr rich shell that forms around the precipitates [8], a feature that has also been observed with 3D atom probe [10] and with small angle X-ray scattering [9].

Fig. 4 shows low magnification HAADF Z-contrast images of the ternary alloy after 4h, 11h and 69h of aging at 450°C. A bright rim can be seen surrounding the precipitates, which arises from the Zr-rich shell. The shell clearly increases in thickness during annealing. The estimated thickness is about 1.5nm at 4h, 4nm at 11h and 6nm at 69h. The latter shell thickness is in good agreement with that estimated from line profile microchemical EDS analysis and high resolution transmission electron microscopy images [8].

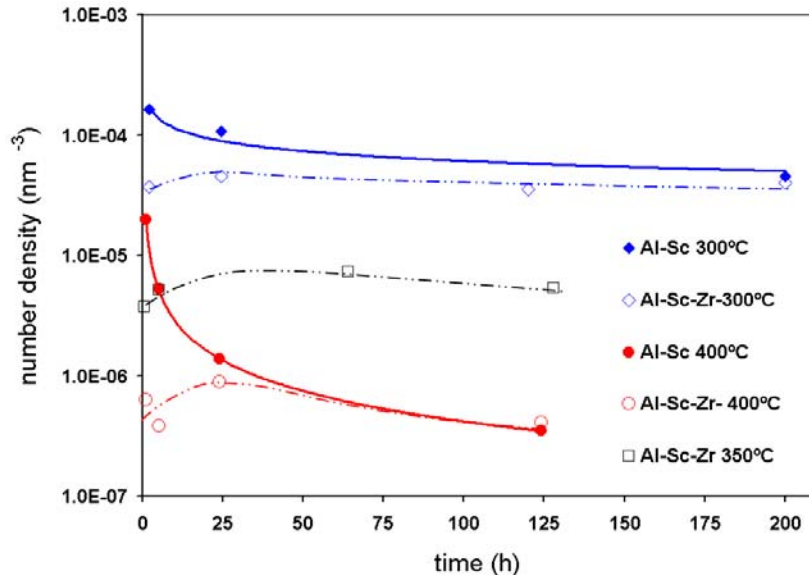


Fig. 3: Number density of Al-Sc and $Al_3(Sc,Zr)$ precipitates as a function of aging and temperature.

Figure 5 shows a high resolution HAADF-STEM image of the particle in fig 4b, its digital diffractogram and an intensity profile across the precipitate edge. It can be seen that the highest contrast occurs at the $Al_3(Sc,Zr)/Al$ matrix interface and that the intensity in the core is substantially higher than in the surrounding Al-rich matrix. It is also apparent that the precipitate is ordered, since only every other $\{002\}$ plane is occupied by the heavy Sc or Zr solute atoms in the $L1_2$ structure, resulting in a fringe periodicity of 0.405nm (Fig. 5). Since the HAADF-STEM image in Fig. 4 is obtained using collection angles between 60 and 100 mrad, the observed contrast can simply be interpreted in terms of differences in atomic number, i.e. the difference in Sc and Zr concentration in the core and the shell of the precipitates. Employing the simple correlation $I \sim Z^\beta$, where I is intensity, Z the atomic number and β a constant, and using

the surrounding Al matrix as an internal standard, it is possible to estimate the Sc and Zr content in the core and shell [11].

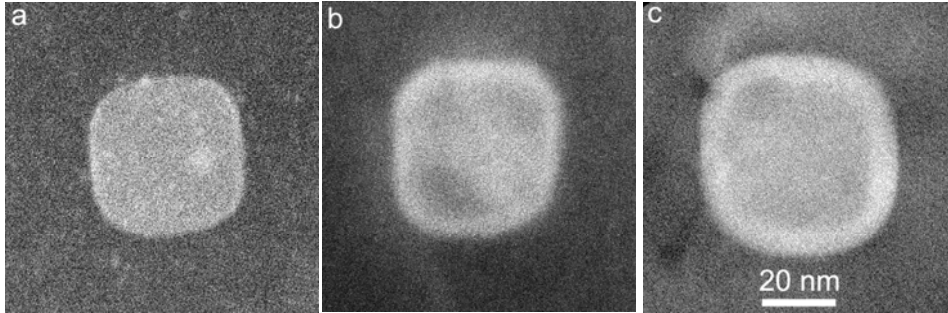


Fig. 4: HAADF Z-contrast images showing the evolution of shell thickness as a function of annealing time at 450°C. (a) 4h, (b) 11h and (c) 69h.

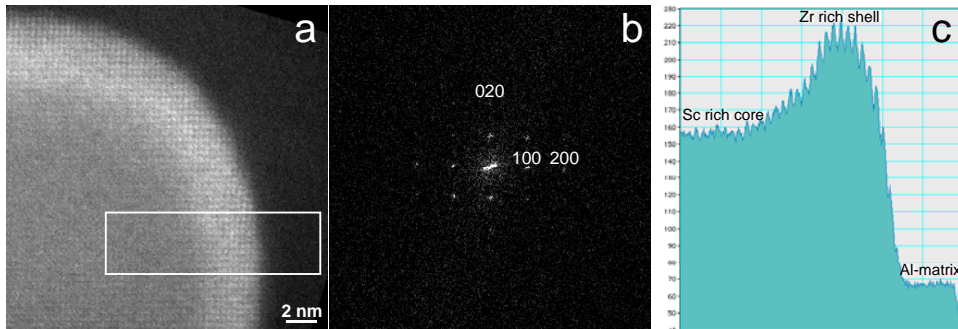


Fig. 5: a) High resolution HAADF Z-contrast image of the particle in figure 4b; b) digital diffractogram showing ordered nature of core/shell precipitate; c) Integrated Z contrast profile from the region indicated in (a)

DSC analyses for binary and ternary alloys are shown in Fig. 6. It is obvious that Sc in the binary alloy precipitates at around 332°C with an enthalpy of $\Delta H \approx 95 \text{ Jmol}^{-1}$, significantly lower than $\text{Al}_3(\text{Sc}_{1-x}\text{Zr}_x)$ in ternary alloy which precipitates at around 370°C with approximately the same enthalpy of $\Delta H \approx 90 \text{ Jmol}^{-1}$.

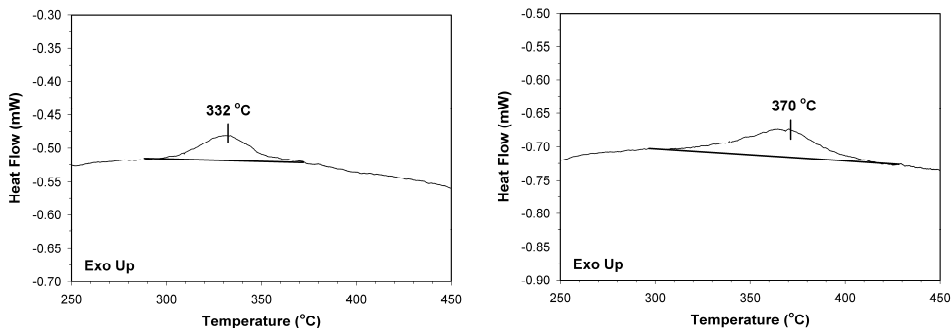


Fig. 5: DSC curves: a) binary Al-Sc alloy; b) ternary Al-Sc-Zr alloy.

These results indicate rapid initial formation of a Sc rich $\text{Al}_3(\text{Sc,Zr})$ core followed by formation of a Zr rich $\text{Al}_3(\text{Zr,Sc})$ shell. The Zr rich shell acts as a diffusion barrier and consequently modifies the growth rate of the Sc rich core.

SUMMARY

We have investigated precipitation kinetics, number density and the distribution, morphology and chemical composition of precipitates in a ternary Al-Sc-Zr alloy during aging at 300, 350, 400 and 450°C, using binary Al-Sc as a baseline.

HAADF STEM imaging and line profile microchemical EDS analysis revealed that in the ternary Al-Sc-Zr alloys the precipitates maintained the ordered L1_2 structure typical of binary alloys and contained both Sc and Zr. The Zr was distributed primarily in a shell surrounded a Sc-rich core. The Zr-rich shell acts as a diffusion barrier and consequently modifies the growth rate of the Sc-rich core, slowing down precipitation kinetics.

REFERENCES

- [1] V.I. Eelagin, V.V. Zakharov and T.D. Rostova, *Metallovedenie I Tericheskaya Obrabotka Metallov*, 7, 57, 1983
- [2] N. Blake and M.A. Hopkins, *J. Mat. Sci.*, 20, 2861, 1985
- [3] V. G. Davidov, T. D. Rostova, V.V. Zakharov, Yu. A. Filatov, V. I. Telagin, *Mat. Sci. Eng.*,
- [4] A 280, 30, 2000.
- [5] Z. Ahmad, *JOM* 55, 35, 2003
- [6] C. B. Fuller, D. N. Seidman and D. C. Dunand, *Acta Mater* 51, 4803, 2003.
- [7] V.I. Eelagin, V.V. Zakharov and T.D. Rostova, *TLS*, 4, 5, 1984.
- [8] V.I. Elagin, V.V. Zakharov, S. G. Pavlenko, T. D. Rostova, *Phys. Met. Metall.*, 60, 88, 1985
- [9] A. Tolley, V. Radmilovic, U. Dahmen, *Scripta Mater.* 52, 621, 2004.
- [10] A. Deschamps, M. Dumont, L. Lae, F. Bley, *Mat. Sci. Forum*, 519-521, 1349, 2006.
- [11] B. Forbord, W. Lefebvre, F. Danoix, H. Hallem, K. Marthinsen, *Scripta Mater* 51, 33, 2004.
- [12] V. Radmilovic, A. Tolley and U. Dahmen, *Microsc. & Microanal.*, 11 (Suppl 2), 1712., 2005.